

# 194367: syenogranite, Ngaturn

## (Pitjantjatjara Supersuite, Musgrave Province)

### Location and sampling

SCOTT (SG 52-6), FINLAYSON (4446)  
MGA Zone 52, 369783E 7166857N

Sampled on 16 May 2008

This sample was collected from low-lying rubbly outcrop, about 31.2 km west-southwest of Mount Muir, 24.3 km east of Domeyer Hill, and 4.7 km northwest of Ngaturn aboriginal site.

### Tectonic unit/relations

The unit sampled is a granite assigned to the 1220–1150 Ma Pitjantjatjara Supersuite (Smithies et al., 2009). The Pitjantjatjara Supersuite comprises syn- to post-tectonic granite magmas emplaced during the Musgrave Orogeny (Smithies et al., 2010; 2011). The Musgrave Orogeny caused intense deformation, widespread granulite-facies reworking, and granitic magmatism of the Pitjantjatjara Supersuite (Edgoose et al., 2004). The absence of clear evidence for significant compressional deformation associated with the prolonged Musgrave Orogeny implies an essentially intracontinental setting (Wade et al., 2008). The Pitjantjatjara granites are ferroan, calc-alkalic to alkali-calcic, emplaced at temperatures  $\geq 1000^\circ\text{C}$ , and include orthopyroxene-bearing charnockites. These rocks formed through melting of a homogenized 1950–1900 Ma source that was refertilized by mantle input (Kirkland et al., 2012).

### Petrographic description

The sample is a syenogranite containing about 45% K-feldspar, 25% quartz, 15% plagioclase + myrmekite, 13% hornblende, 1% opaque oxide minerals and accessory garnet, biotite, epidote, apatite, titanite, allanite, and zircon. The texture is allotriomorphic granular, with most quartz and feldspar grains and mafic aggregates (hornblende–opaque oxide  $\pm$  biotite, apatite, epidote, titanite, and zircon) less than 2 mm long. Very minor myrmekite occurs in plagioclase and there is weak clay alteration in feldspar grains.

### Zircon morphology

Zircons from this sample are colourless to dark brown or opaque, and mainly euhedral. The crystals are up to

500  $\mu\text{m}$  long, and equant to elongate, with aspect ratios up to 6:1. In cathodoluminescence (CL) images, most crystals exhibit concentric zoning, and many contain high-uranium, metamict zones. A CL image of representative zircons is shown in Figure 1.

### Analytical details

This sample was analysed over two sessions, on 29–30 January and 30–31 January 2009, using SHRIMP-B. Analyses 1.1 to 14.1 (spot numbers 1–14) were obtained during the first session, together with 12 analyses of the Temora standard, of which 11 analyses indicated an external spot-to-spot (reproducibility) uncertainty of 1.22% ( $1\sigma$ ) and a  $^{238}\text{U}/^{206}\text{Pb}^*$  calibration uncertainty of 0.44% ( $1\sigma$ ). Analyses 15.1 to 20.1 (spot numbers 15–20) were obtained during the second session, together with 12 analyses of the Temora standard, which indicated an external spot-to-spot (reproducibility) uncertainty of 1.51% ( $1\sigma$ ) and a  $^{238}\text{U}/^{206}\text{Pb}^*$  calibration uncertainty of 0.53% ( $1\sigma$ ). Calibration uncertainties are included in the errors of  $^{238}\text{U}/^{206}\text{Pb}^*$  ratios and dates listed in Table 1. Common-Pb corrections were applied to all analyses using contemporaneous isotopic compositions determined according to the model of Stacey and Kramers (1975).

### Results

Twenty analyses were obtained from 20 zircons. Results are listed in Table 1, and shown in concordia diagrams (Figs 2 and 4), and an X–Y correlation plot (Fig. 3).

### Interpretation

The analyses are concordant to slightly discordant. The analyses yield  $^{207}\text{Pb}^*/^{206}\text{Pb}^*$  dates that correlate with their common-Pb contents ( $f_{204}$ , Fig. 3), indicating that corrections using  $^{204}\text{Pb}$  are inaccurate for some or all of these analyses. The date for this sample is therefore determined from the intersection with the concordia curve of a regression through uncorrected data (Fig. 4), anchored at contemporaneous initial Pb ( $^{207}\text{Pb}/^{206}\text{Pb} = 0.9222$  at 1160 Ma; Stacey and Kramers, 1975). The analyses define a single coherent group, based on their  $^{207}\text{Pb}/^{206}\text{Pb}$  and  $^{238}\text{U}/^{206}\text{Pb}$  ratios.

Group I comprises 20 analyses (Table 1), for which the regression intersects the concordia curve at  $1159 \pm 7$  Ma (MSWD = 1.3).

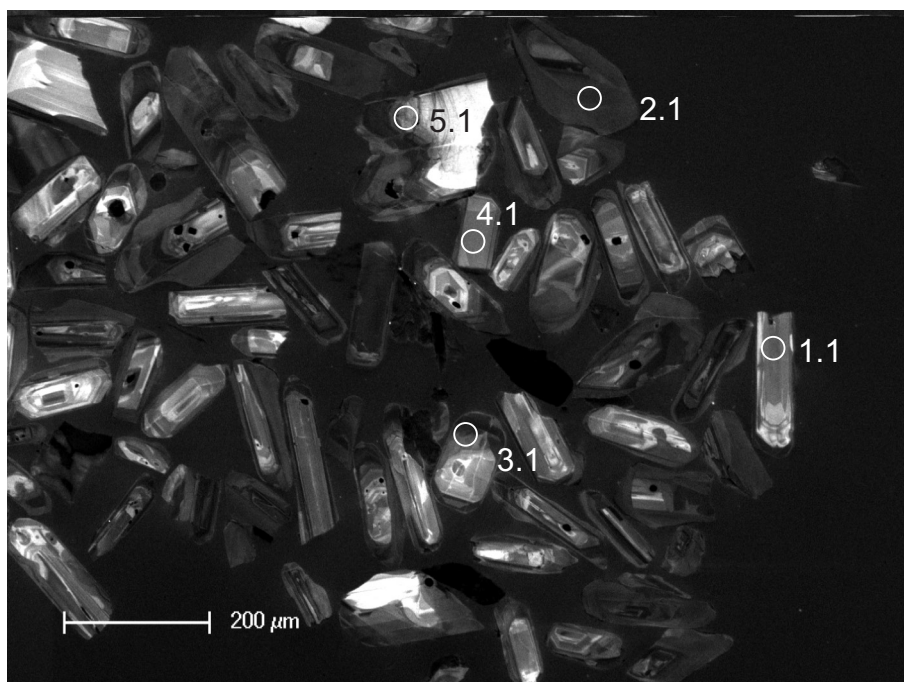


Figure 1. Cathodoluminescence image of representative zircons from sample 194367: syenogranite, Ngaturn. Numbered circles indicate the approximate positions of analysis sites.

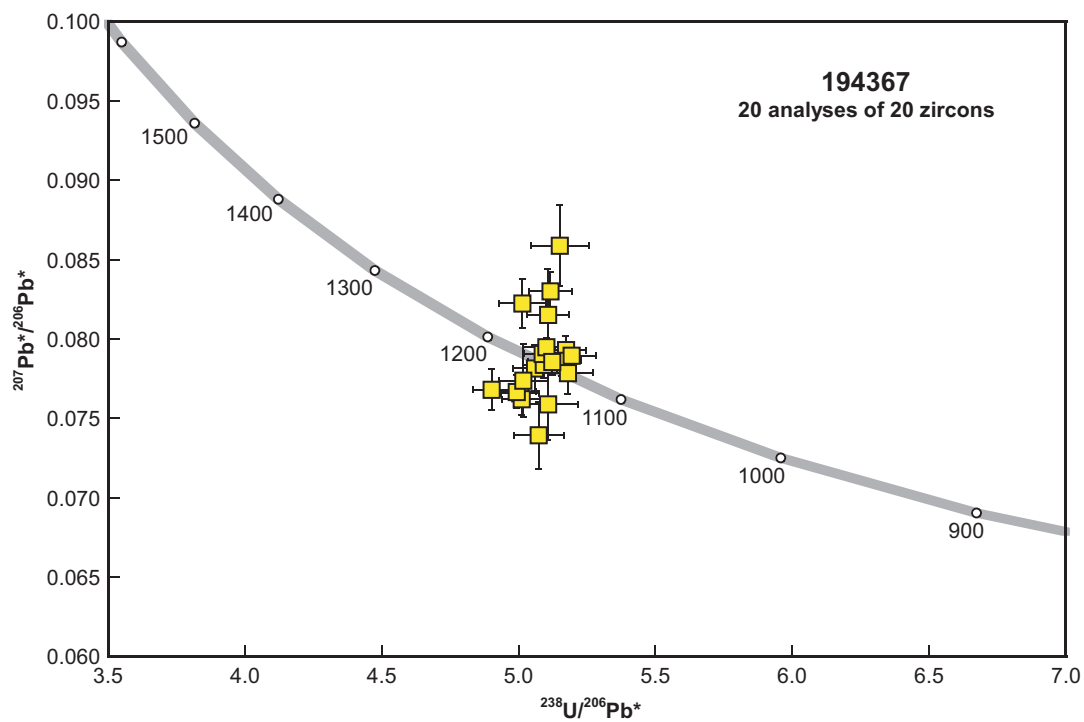
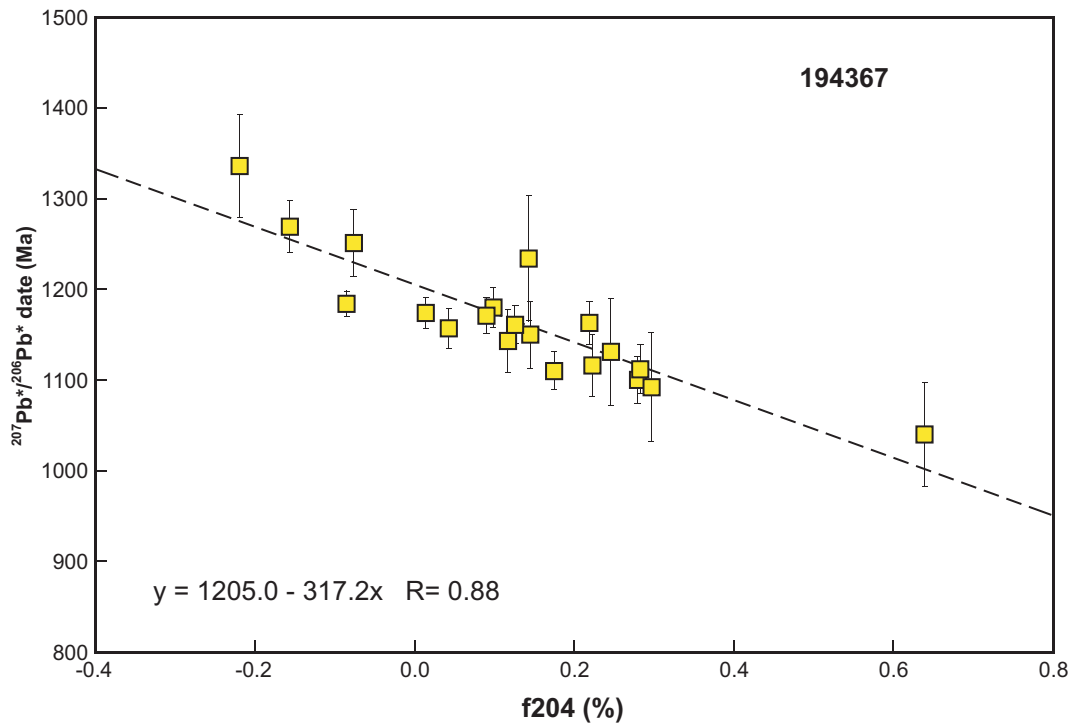


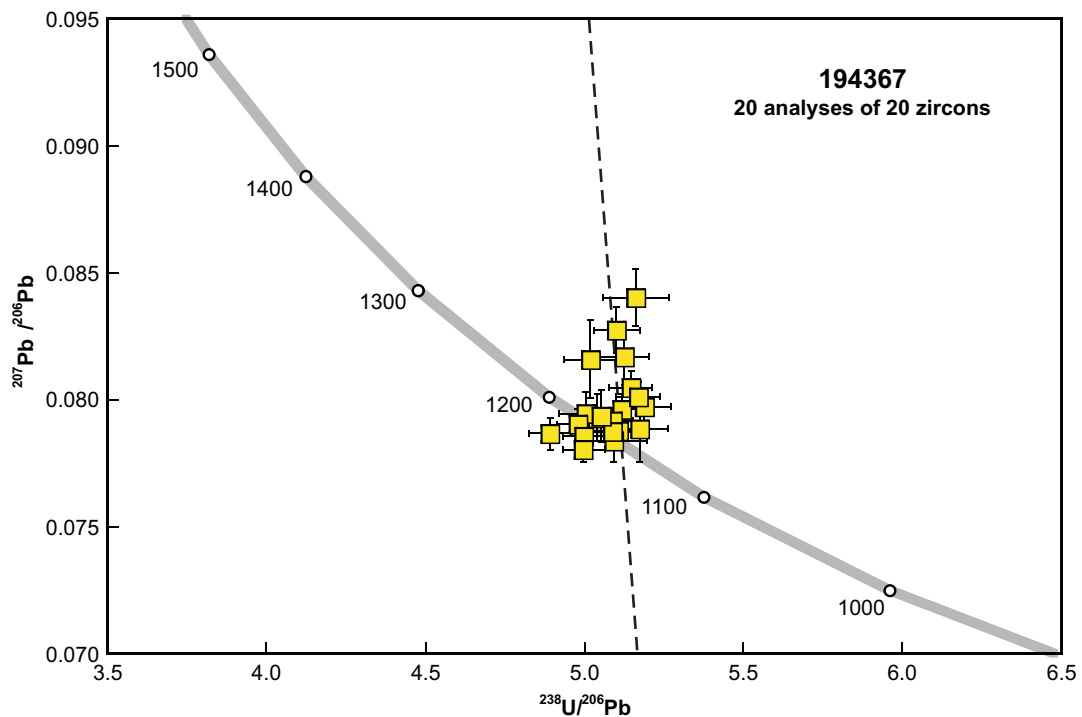
Figure 2. U-Pb analytical data for sample 194367: syenogranite, Ngaturn. Yellow squares indicate Group I (magmatic zircons).

Table 1. Ion microprobe analytical results for zircons from sample 194367: syenogranite, Ngatatum

| Group ID | Spot no. | Grain. spot | <sup>238</sup> U (ppm) | <sup>232</sup> Th (ppm) | $\frac{^{232}\text{Th}}{^{238}\text{U}}$ | f204 (%) | $^{238}\text{U}/^{206}\text{Pb} \pm 1\sigma$ | $^{207}\text{Pb}/^{206}\text{Pb} \pm 1\sigma$ | $^{238}\text{U}/^{206}\text{Pb}^* \pm 1\sigma$ | $^{207}\text{Pb}^*/^{206}\text{Pb}^* \pm 1\sigma$ | $^{238}\text{U}/^{206}\text{Pb}^*$ date (Ma) $\pm 1\sigma$ | $^{207}\text{Pb}^*/^{206}\text{Pb}^*$ date (Ma) $\pm 1\sigma$ | Disc. (%) |         |      |    |      |    |      |
|----------|----------|-------------|------------------------|-------------------------|--|----------|--|---|--|---|--|---|-----------|---------|------|----|------|----|------|
| I        | 20       | 20.1        | 98                     | 231                     | 2.44                                     | 0.639    | 5.041  | 0.087   | 0.07930  | 0.00092   | 5.074  | 0.092   | 0.07394   | 0.00210 | 1160 | 23 | 1040 | 57 | 11.5 |
| I        | 13       | 13.1        | 131                    | 140                     | 1.10                                     | 0.297    | 5.093  | 0.104   | 0.07837  | 0.00080   | 5.108  | 0.108   | 0.07588   | 0.00226 | 1153 | 27 | 1092 | 60 | 5.6  |
| I        | 8        | 8.1         | 182                    | 159                     | 0.90                                     | 0.280    | 4.998  | 0.066   | 0.07856  | 0.00061   | 5.012  | 0.070   | 0.07620   | 0.00100 | 1173 | 18 | 1100 | 26 | 6.6  |
| I        | 3        | 3.1         | 282                    | 286                     | 1.05                                     | 0.175    | 4.997  | 0.065   | 0.07805  | 0.00049   | 5.006  | 0.068   | 0.07658   | 0.00081 | 1174 | 18 | 1110 | 21 | 5.8  |
| I        | 14       | 14.1        | 205                    | 203                     | 1.02                                     | 0.283    | 4.980  | 0.066   | 0.07905  | 0.00060   | 4.994  | 0.070   | 0.07666   | 0.00104 | 1177 | 18 | 1112 | 27 | 5.8  |
| I        | 11       | 11.1        | 183                    | 205                     | 1.16                                     | 0.223    | 4.891  | 0.065   | 0.07867  | 0.00062   | 4.902  | 0.069   | 0.07680   | 0.00130 | 1197 | 19 | 1116 | 34 | 7.2  |
| I        | 19       | 19.1        | 114                    | 225                     | 2.04                                     | 0.246    | 5.005  | 0.084   | 0.07945  | 0.00086   | 5.018  | 0.090   | 0.07738   | 0.00230 | 1172 | 23 | 1131 | 59 | 3.6  |
| I        | 16       | 16.1        | 171                    | 156                     | 0.95                                     | 0.117    | 5.175  | 0.086   | 0.07885  | 0.00132   | 5.181  | 0.091   | 0.07786   | 0.00135 | 1138 | 22 | 1143 | 35 | 0.5  |
| I        | 4        | 4.1         | 64                     | 184                     | 2.96                                     | 0.145    | 5.053  | 0.075   | 0.07936  | 0.00103   | 5.060  | 0.079   | 0.07814   | 0.00145 | 1163 | 20 | 1150 | 37 | 1.1  |
| I        | 9        | 9.1         | 248                    | 278                     | 1.16                                     | 0.043    | 5.089  | 0.071   | 0.07874  | 0.00053   | 5.092  | 0.074   | 0.07838   | 0.00086 | 1156 | 18 | 1157 | 22 | 0.0  |
| I        | 18       | 18.1        | 238                    | 259                     | 1.13                                     | 0.126    | 5.117  | 0.082   | 0.07962  | 0.00060   | 5.123  | 0.087   | 0.07856   | 0.00084 | 1149 | 21 | 1161 | 21 | 1.0  |
| I        | 6        | 6.1         | 192                    | 159                     | 0.85                                     | 0.219    | 5.146  | 0.068   | 0.08049  | 0.00061   | 5.157  | 0.072   | 0.07864   | 0.00096 | 1142 | 17 | 1163 | 24 | 1.8  |
| I        | 17       | 17.1        | 228                    | 156                     | 0.71                                     | 0.090    | 5.189  | 0.083   | 0.07972  | 0.00063   | 5.194  | 0.088   | 0.07896   | 0.00081 | 1135 | 21 | 1171 | 20 | 3.1  |
| I        | 10       | 10.1        | 319                    | 479                     | 1.55                                     | 0.014    | 5.088  | 0.065   | 0.07918  | 0.00048   | 5.089  | 0.069   | 0.07906   | 0.00067 | 1156 | 17 | 1174 | 17 | 1.5  |
| I        | 2        | 2.1         | 216                    | 157                     | 0.75                                     | 0.099    | 5.169  | 0.068   | 0.08013  | 0.00058   | 5.174  | 0.072   | 0.07930   | 0.00087 | 1139 | 17 | 1180 | 22 | 3.4  |
| I        | 15       | 15.1        | 287                    | 319                     | 1.15                                     | 0.085    | 5.107  | 0.081   | 0.07878  | 0.00055   | 5.102  | 0.085   | 0.07949   | 0.00057 | 1154 | 21 | 1184 | 14 | 2.6  |
| I        | 7        | 7.1         | 108                    | 189                     | 1.81                                     | 0.143    | 5.101  | 0.072   | 0.08274  | 0.00088   | 5.108  | 0.078   | 0.08152   | 0.00288 | 1152 | 19 | 1234 | 69 | 6.6  |
| I        | 5        | 5.1         | 94                     | 201                     | 2.21                                     | 0.076    | 5.018  | 0.083   | 0.08159  | 0.00154   | 5.014  | 0.086   | 0.08224   | 0.00156 | 1172 | 22 | 1251 | 37 | 6.3  |
| I        | 12       | 12.1        | 66                     | 181                     | 2.83                                     | 0.156    | 5.125  | 0.077   | 0.08168  | 0.00109   | 5.117  | 0.080   | 0.08300   | 0.00123 | 1151 | 20 | 1269 | 29 | 9.3  |
| I        | 1        | 1.1         | 63                     | 200                     | 3.28                                     | 0.219    | 5.162  | 0.103   | 0.08402  | 0.00113   | 5.151  | 0.107   | 0.08588   | 0.00253 | 1144 | 26 | 1336 | 57 | 14.4 |



**Figure 3.** Correlation between  $^{207}\text{Pb}^*/^{206}\text{Pb}^*$  age (corrected for common Pb using measured  $^{204}\text{Pb}$ ) and  $f_{204}$  for sample 194367: syenogranite, Ngaturn. The dashed line indicates a regression through data in Group I, and the equation of the best-fit line is shown. R is Pearson's correlation coefficient. Symbols as in Figure 2.



**Figure 4.** U-Pb analytical data, not corrected for common Pb, for sample 194367: syenogranite, Ngaturn. The dashed line indicates a regression from initial Pb, through data in Group I. Symbols as in Figure 2.

The date of  $1159 \pm 7$  Ma for the 20 analyses in Group I is interpreted as the magmatic crystallization age of the granite.

## References

- Edgoose, CJ, Scrimgeour, IR and Close, DF 2004, Geology of the Musgrave Block, Northern Territory: Northern Territory Geological Survey, Report 15, 48p.
- Kirkland, CL, Smithies, RH, Woodhouse, A, Howard, H, Wilson, AC, Belousova, EA, Cliff, JB, Murphy, R, Spaggiari, CV 2012, A multi-isotopic approach to the crustal evolution of the west Musgrave province, Central Australia: Geological Survey of Western Australia Report 115, 53p.
- Smithies, RH, Howard, HM, Evins, PM, Kirkland, CL, Bodorkos, S and Wingate, MTD 2009, The west Musgrave Complex — some new geological insights from recent mapping, geochronology, and geochemical studies: Geological Survey of Western Australia, Record 2008/19, 20p.
- Smithies, RH, Howard, HM, Evins, PM, Kirkland, CL, Kelsey, DE, Hand, M, Wingate, MTD, Collins, AS, Belousova, E and Allchurch, S 2010, Geochemistry, geochronology, and petrogenesis of Mesoproterozoic felsic rocks in the west Musgrave Province, central Australia, and implications for the Mesoproterozoic tectonic evolution of the region: Geological Survey of Western Australia, Report 106, 73p.
- Smithies, RH, Howard, HM, Evins, PM, Kirkland, CL, Kelsey, DE, Hand, M, Wingate, MTD, Collins, AS and Belousova, E 2011, High-temperature granite magmatism, crust-mantle interaction and the mesoproterozoic intracontinental evolution of the Musgrave Province, central Australia: *Journal of Petrology*, v. 52, p. 931–958.
- Stacey, JS and Kramers, JD 1975, Approximation of terrestrial lead isotope evolution by a two-stage model: *Earth and Planetary Science Letters*, v. 26, p. 207–221.
- Wade, B, Kelsey, D, Hand, M and Barovich, K 2008, The Musgrave Province: stitching north, west and south Australia: *Precambrian Research*, v. 166, p. 370–386.

## Recommended reference for this publication

Kirkland, CL, Wingate, MTD and Evins, PM 2013, 194367: syenogranite, Ngaturn; Geochronology Record 1134: Geological Survey of Western Australia, 5p.

Data obtained: 31 January 2009

Data released: 30 June 2013